



# Ultrarapid exhumation of ultrahigh-pressure diamond-bearing metasedimentary rocks of the Kokchetav Massif, Kazakhstan?☆

Bradley R. Hacker<sup>a,\*</sup>, Andrew Calvert<sup>a</sup>, R.Y. Zhang<sup>b</sup>, W. Gary Ernst<sup>b</sup>, J.G. Liou<sup>b</sup>

<sup>a</sup>Department of Geological Sciences, University of California, Santa Barbara, CA 93106-9630, USA

<sup>b</sup>Department of Geological and Environmental Sciences, Stanford University, Stanford, CA 94305-2115, USA

## Abstract

The diamond-bearing, ultrahigh-pressure Kokchetav Massif recrystallized at eclogite-facies conditions deep in the mantle at 180-km depth at  $535 \pm 3$  Ma, and yet new  $^{40}\text{Ar}/^{39}\text{Ar}$  ages suggest that it may have been exhumed to crustal depths (as indicated by closure of mica to Ar loss) by  $\sim 529$  Ma. These data indicate a possible exhumation rate of tens of kilometers per million years, i.e., a rate that is comparable to rates of horizontal plate motion and subduction.

© 2003 Elsevier B.V. All rights reserved.

**Keywords:** Kokchetav Massif; Ultrahigh-pressure metamorphism; Excess argon; Exhumation rate

## 1. Introduction

The Kokchetav Massif, Kazakhstan (Fig. 1), is a large ( $\sim 10\text{--}15 \times 150$  km) ultrahigh-pressure terrane, distinctive because of the very unusual widespread occurrence of metamorphic diamond (e.g., Dobretsov et al., 1998; Maruyama and Parkinson, 2000; Sobolev et al., 1990) and coesite (Katayama et al., 2000; Parkinson, 2000) that formed as a result of subduction of a continental margin or microcontinent. In spite of this, its geological relationships are relatively poorly known because of geographic inaccessibility and poor outcrop. A spate of recent studies (see references quoted in this article) has, however, produced an excellent structural and petrological assessment of the

Kokchetav Massif. This paper reports new  $^{40}\text{Ar}/^{39}\text{Ar}$  geochronology to complement the petrological and structural investigations and provide new time constraints on the history of this remarkable group of rocks. Unless otherwise noted, quoted uncertainties for radiometric ages are  $2\sigma$ .

## 2. Geology of the Kokchetav Massif

The Kokchetav Massif consists of dominantly continental rocks that have most recently been divided into four flat-lying, fault-bounded, high-pressure to ultrahigh-pressure units with an aggregate thickness of  $\sim 2$  km (Maruyama and Parkinson, 2000). Early subhorizontal structures characterized by intrafolial isoclinal folds are overprinted by late steep structures (Kaneko et al., 2000; Yamamoto et al., 2000).

Unit I, the structurally lowest unit, is composed of amphibolite, orthogneiss, and pelitic schist recrystallized at amphibolite-facies conditions of  $700\text{--}815$  °C,

☆ Supplementary data associated with this article can be found at [doi:10.1016/S0024-4937\(03\)00092-6](https://doi.org/10.1016/S0024-4937(03)00092-6).

\* Corresponding author. Tel.: +1-805-893-7952; fax: +1-805-893-2314.

E-mail address: [hacker@geology.ucsb.edu](mailto:hacker@geology.ucsb.edu) (B.R. Hacker).

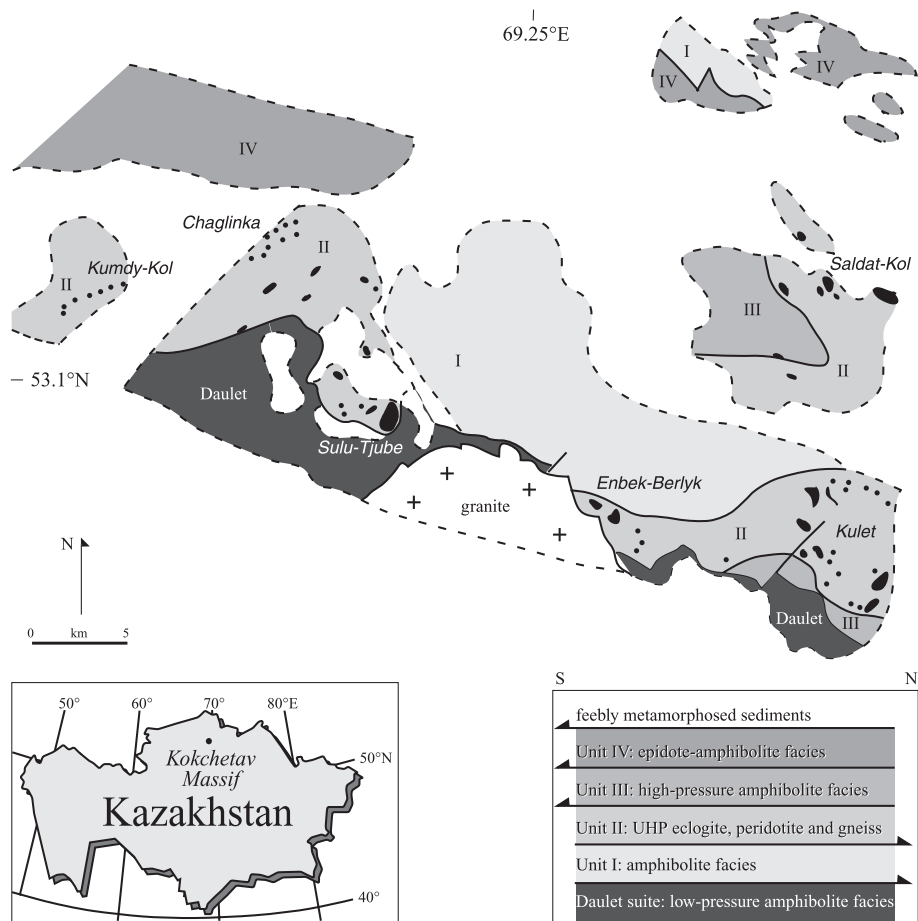


Fig. 1. Map distribution of Units I–IV and eclogite bodies (black) of Kokchetav Massif (after Kaneko et al., 2000). Insets show location of Massif and schematic structural section. Poor exposure (white indicates areas of no exposure) dictates that the map relations at this scale are necessarily simplified. Further details of the field relations are best obtained from, for example, Kaneko et al. (2000) and Yamamoto et al. (2000).

1.2–1.3 GPa (Masago, 2000; Ota et al., 2000). Unit II, pelitic–psammitic gneiss and whiteschist, with variably retrogressed eclogite and minor pods of garnet peridotite, experienced peak metamorphism at 780–1000 °C, 3.7–6.0(?) GPa (Okamoto et al., 2000). Unit II contains the remarkable microdiamonds as inclusions in garnet, zircon, and clinopyroxene from dolomitic marble, clinopyroxene-bearing garnet quartzite, and garnet–biotite paragneiss; coesite as inclusions in eclogite, paragneiss, and whiteschist; and clinopyroxene with as much as 1.0 wt.% K<sub>2</sub>O in gneiss, marble, and eclogite (Okamoto et al., 2000). Unit III, chiefly interlayered orthogneiss and amphibolite (blocks of UHP eclogite at the base of Unit III may have been

derived from Unit II), was metamorphosed at 730–750 °C, 1.1–1.4 GPa (Ota et al., 2000). Unit IV, the structurally highest unit, consists of quartzose meta-sediments with minor amphibolite; it experienced epidote-amphibolite facies P–T conditions of 400–500 °C, 0.9 GPa (Masago, 2000). Units I, II, and III all show a late amphibolite-facies overprint at 570–680 °C, 0.7–1.3 GPa, equivalent to the peak metamorphism of Unit IV (Masago, 2000; Ota et al., 2000).

Unit I shows top-N(W) sense-of-shear indicators (mica fish, shear bands, etc.) (Yamamoto et al., 2000), whereas Units III (Yamamoto et al., 2000) and IV (Kaneko et al., 2000) contain top-S shear indicators. Because ultrahigh-pressure Unit II overlies high-pres-

sure Unit I with top-N(W) sense of shear and underlies high- to medium-pressure Units III and IV with show top-S(E) sense of shear, Unit II is interpreted to have been exhumed upward and northward within a channel bounded by lower pressure rocks to the north and south (Maruyama and Parkinson, 2000).

These high-pressure to ultrahigh-pressure rocks are tectonically overlain and underlain by rocks metamorphosed at normal crustal pressures and temperatures. Unit I overlies the Daulet Suite, pelitic–psammitic rocks recrystallized at low pressures (500–650 °C, 0.2–0.3 GPa (Terabayashi, 1999)), along a gently N-dipping fault with top-N shear bands (Ishikawa et al., 2000). Unit IV is overlain by feebly metamorphosed clastic and carbonate rocks along a gently inclined normal fault with top-S motion (Kaneko et al., 2000). Unmetamorphosed and undeformed granitic plutons intrude Units I, II, III, and the Daulet Suite (Ishikawa et al., 2000); some of these are reportedly 420–460 Ma (Dobretsov et al., 1998) and 515–517 Ma (Borisova et al., 1995), but insufficient data are available to evaluate these ages.

### 3. Geochronology

High-resolution geochronologic data for the Kokchetav Massif are rather sparse. The first sensitive high-resolution ion microprobe (SHRIMP) U/Pb analyses of Kokchetav zircons with diamond inclusions yielded a mean age of  $530 \pm 7$  Ma (Claoue-Long et al., 1991). Katayama et al. (2001) subsequently obtained more SHRIMP data on zircons from diamond-bearing gneiss, diamond-free gneiss, and a coesite-bearing eclogite. After rejecting one anomalously old age, they reported a  $^{238}\text{U}/^{206}\text{Pb}$  mean age of  $537 \pm 9$  Ma for grain cores and mantles with ultrahigh-pressure mineral inclusions; after excluding two anomalously young ages, they reported a  $^{238}\text{U}/^{206}\text{Pb}$  mean age of  $507 \pm 8$  Ma for grain rims that contain low-P mineral inclusions such as graphite, quartz, and chlorite. Note that *all* of their core and rim ages (aside from the three they excluded) fit a single population with an age of  $519.8 \pm 6.4$  Ma (MSWD=1.4), and *on a statistical basis*, cannot be separated into two populations. Zircon ages from ultrahigh-pressure rocks are often difficult to tie directly to the time of ultrahigh-pressure metamorphism (e.g., Hacker et al., 1998), but the textural

observations of ultrahigh-pressure mineral inclusions by Katayama et al. (2001) are definitive.

Sm/Nd or Lu/Hf analyses of ultrahigh-pressure phases are a more direct means of assessing time at peak pressure, but they may be complicated by zoning (Brueckner et al., 1996) or later hydrothermal

Table 1  
Sample descriptions; all from ultrahigh-pressure Unit II

Sample	Location	Rock description
95K-2	Kumdy–Kol	garnet–biotite gneiss. Garnet porphyroblasts of 1- to 4-mm set in a matrix of quartz, minor plagioclase, and biotite
95K-3	Kumdy–Kol	similar to 95K-2
95K-5b	Kumdy–Kol	quartz-rich eclogite with >50% garnet, 30% quartz, hornblende replacement of clinopyroxene, and minor rutile
95K-5c	Kumdy–Kol	quartz–muscovite–plagioclase–K-feldspar(?) gneiss. With minor garnet and apatite
95K-5e	Kumdy–Kol	garnet–muscovite–kyanite–quartz schist with minor feldspar, tourmaline, rutile, and zircon. Secondary biotite and chlorite replace garnet and kyanite. Strong foliation
95K-7	Kumdy–Kol	diopside-bearing dolomitic marble
95K-8a'	Kumdy–Kol	similar to 95K-5E, but garnet is coarser (1.5–5 mm)
95K-11a	Kumdy–Kol	diamond-bearing gneiss with garnet, muscovite, biotite, quartz, plagioclase, and minor tourmaline. Diamonds are rare inclusions in garnet
95K-11c	Kumdy–Kol	garnet–biotite–quartz schist. Garnets (>10 vol.%) contain many inclusions of biotite and quartz; some are atoll shaped
95K-21f	Kulet	garnet–muscovite–biotite–quartz schist with minor rutile; strong deformation. Strong foliation; garnets are fractured
A-12	Kumdy–Kol?	garnet–kyanite–muscovite–biotite metasediment
KZ-5	Kumdy–Kol	eclogite partially retrogressed to amphibolite
KZ-7	Kumdy–Kol	garnet–muscovite–plagioclase–quartz orthogneiss
KZ-10	Kumdy–Kol	quartzose eclogite partially retrogressed to biotite-bearing amphibolite
KZ-17	Sulu–Tjube	eclogite partially retrogressed to zoisite-bearing amphibolite
KZ-24	Kulet	pyrope–talc–kyanite schist with minor biotite

Table 2  
Summary of  $^{40}\text{Ar}/^{39}\text{Ar}$  data

Sample	Mineral	Size ( $\mu\text{m}$ )	Mass (mg)	TFA	WMPA <sup>a</sup>	IA <sup>b</sup>	$^{40}\text{Ar}/^{36}\text{Ar}$	MSWD	Steps used	% used
95K-2	bio	90–125	0.39	483.9 $\pm$ 0.9	none	n/a	n/a	n/a	n/a	n/a
95K-3	bio	180–250	0.35	502.8 $\pm$ 0.9	<b>510.3 <math>\pm</math> 0.9</b>	509.8 $\pm$ 1.1	467 $\pm$ 165	0.28	22–31/36	38
	mus	180–250	0.55	505.1 $\pm$ 0.9	<b>506.6 <math>\pm</math> 0.9</b>	<i>505.9 <math>\pm</math> 1.1</i>	333 $\pm$ 30	2.6	7–31/41	70
95K-5b	hbl	125–180	2.00	643.4 $\pm$ 1.1	none	none	n/a	n/a	n/a	n/a
95K-5c	mus	355–500	0.45	526.0 $\pm$ 0.9	<b>525.3 <math>\pm</math> 0.9</b>	524.6 $\pm$ 1.2	398 $\pm$ 99	1	12–22/39	33
95K-5e	mus	355–500	0.45	531.0 $\pm$ 0.9	<b>529.4 <math>\pm</math> 1.0</b>	529.6 $\pm$ 1.5	285 $\pm$ 81	0.42	16–22/42	48
95K-7	cpx	~ 400	6.7	748.9 $\pm$ 6.0	none	none	n/a	n/a	n/a	n/a
95K-8a'	mus	355–500	0.30	509.8 $\pm$ 0.9	<b>509.4 <math>\pm</math> 0.9</b>	508.9 $\pm$ 1.0	324 $\pm$ 18	1.2	5–34/36	90
95K-11a	bio	106–150	0.55	502.1 $\pm$ 0.9	<b>510.8 <math>\pm</math> 0.9</b>	510.1 $\pm$ 1.7	451 $\pm$ 199	0.31	24–28/30	18
95K-11c	bio	180–250	0.48	506.7 $\pm$ 0.9	<b>511.4 <math>\pm</math> 0.9</b>	510.2 $\pm$ 1.0	503 $\pm$ 62	2.1	5–29/31	71
95K-21f	bio	180–250	0.45	422.4 $\pm$ 0.8	none	none	n/a	n/a	n/a	n/a
	mu	180–250	0.48	495.6 $\pm$ 0.9	~ <b>499 <math>\pm</math> 3</b>	none	n/a	n/a	9–34/35	74
A-12	mus	355–500	0.26	510.0 $\pm$ 0.9	<b>508.9 <math>\pm</math> 0.9</b>	509.1 $\pm$ 1.0	290 $\pm$ 20	1.5	5–27/28	82
KZ-5	hbl	125–180	2.00	653.0 $\pm$ 1.1	~ <b>651 <math>\pm</math> 7</b>	<b>664 <math>\pm</math> 2</b> <b>relict age?</b>	< 0	0.83	11–23/33	52
KZ-7	mus	250–300	0.47	505.3 $\pm$ 0.9	<b>506.9 <math>\pm</math> 0.9</b>	<i>507.2 <math>\pm</math> 1.1</i>	274 $\pm$ 36	<b>2.7</b>	5–32/41	85
KZ-10	bio	125–180	0.21	521.1 $\pm$ 0.9	<b>528.3 <math>\pm</math> 0.9</b>	523.5 $\pm$ 2.0	1465 $\pm$ 1296	1	7–25/27	76
KZ-17	hbl	125–180	2.80	512.0 $\pm$ 0.9	none	none	n/a	n/a	n/a	n/a
KZ-24	bio	180–250	0.25	501.8 $\pm$ 1.1	<b>504.7 <math>\pm</math> 1.0</b>	see text	none	none	20–23/29	14

Preferred ages are in bold.

Uncertainties in table are  $\pm 1\sigma$ , whereas  $\pm 2\sigma$  is quoted in the text.

<sup>a</sup> Italics indicate weighted mean ages (WMA); remainder are weighted mean plateau ages (WMPA).

<sup>b</sup> Isochron ages (IA) in italics are poor fits that have MSWD greater than expected.

exchange (Shatsky et al., 1999b). About half the mineral-whole rock  $^{147}\text{Sm}/^{144}\text{Nd}$  and  $^{143}\text{Nd}/^{144}\text{Nd}$  ratios reported from Kokchetav (Shatsky et al., 1993; Shatsky et al., 1999a,b) are not colinear, as is common for high-pressure rocks, indicating a lack of equilibrium or subsequent alteration. Garnets and clinopyroxenes from two eclogites from the diamondiferous Kumdy–Kol area, however, yielded a good-fitting Sm/Nd isochron of  $535 \pm 3$  Ma (Shatsky et al., 1999b). Pooling the two SHRIMP determinations with the Sm/Nd age yields a mean age of  $534.5 \pm 5.2$  (MSWD = 0.26). That the SHRIMP ages are concordant with the Sm/Nd age implies that the zircon ages indeed reflect zircon growth at ultrahigh pressure.

To constrain the timing and path of exhumation of the Kokchetav ultrahigh-pressure rocks, we undertook  $^{40}\text{Ar}/^{39}\text{Ar}$  resistance furnace dating of multigrain separates of hornblende, K-white mica (henceforth referred to as “muscovite”), biotite, and K-bearing diopside. All the samples we analyzed are from Unit II; all are from the Kumdy–Kol area (Fig. 1), except for two from the Kulet area and one from the Sulu–Tjube area. The samples include mafic eclogites,

quartzose eclogites, diamond-bearing gneiss, diamond-free gneiss, and dolomitic marble (Table 1). The results are summarized in Table 2 and reported in full in the appendix.<sup>1</sup>

Unless otherwise mentioned, analytical techniques followed Calvert et al. (1999). We calculate weighted mean plateau ages (WMPA) from consecutive step ages that make up >50% of the released  $^{39}\text{Ar}$  and are statistically equivalent at the 95% confidence interval. We calculate weighted mean ages (WMA) from consecutive step ages that are not statistically equivalent at the 95% confidence interval, but for which a part of the spectrum is not hump shaped, saddle shaped, crankshaft shaped, or composed of serially increasing or decreasing step ages; these “non-flat” spectrum types often indicate excess Ar, in vacuo degassing of more than one mineral or domain, or recoil of  $^{39}\text{Ar}^{\text{K}}$ .

Interpreting the  $^{40}\text{Ar}/^{39}\text{Ar}$  ages of high-pressure minerals is often difficult because of the presence of excess  $^{40}\text{Ar}$  or other factors (e.g., Hacker and Wang, 1995; Li et al., 1994; Scaillet, 1998). Samples may

<sup>1</sup> See Appendix in the online version of this article.

yield plateau that are geochronologically meaningless, either because of in vacuo homogenization or homogeneously distributed excess Ar (e.g., Foland, 1983). Mixed age populations (e.g., Wijbrans and McDougall, 1986), recoil of  $^{39}\text{Ar}^{\text{K}}$  in chloritized biotite (Lo and Onstott, 1989; Ruffet et al., 1991), or contamination by other phases (e.g., Rex et al., 1993) can produce complexly shaped spectra. Laser microprobe  $^{40}\text{Ar}/^{39}\text{Ar}$  dating of grains can help resolve some of these issues by detailing the spatial distribution of Ar isotopes within grains (e.g., Arnaud and Kelley, 1995; Giorgis et al., 2000; Scaillet, 1998). In the absence of laser microprobe dating, however, there are several means by which one can assess the meaning of spectra. (1) Analyzing the same minerals from different rock types. Eclogites often exhibit the most excess  $^{40}\text{Ar}$ , presumably because their  $^{40}\text{Ar}$  content is small relative to the typically K-rich surrounding gneisses. If different rocks from the same locality (e.g., paragneiss and eclogite) yield different spectra, one or both spectra may be suspect. (2) Analyzing different grains or groups of grains from a single sample. Because excess  $^{40}\text{Ar}$  is inhomogeneously distributed, different (groups of) grains with excess  $^{40}\text{Ar}$  can yield quite different spectra, whereas different groups of grains without excess  $^{40}\text{Ar}$  should yield similar spectra. (3) Spectrum shape—either saddle- or hump-shaped—is often diagnostic of excess  $^{40}\text{Ar}$  (Harrison and McDougall, 1981). (4) Analyzing a suite of minerals or suite of grain sizes from a single sample should yield a range of ages that fall in a sequence dictated by closure temperature. If the suite does not produce such a sequence, some ages may be suspect. (5) Analyzing multiple minerals with different isotopic systems to assess whether the sequence of ages follows the expected sequence of closure temperatures. See, for example, Tonarini et al. (1993), Li et al. (1994), and El-Shazly et al. (2001) for examples of some of these tests.

Six Kokchetav micas (samples 95K-3 muscovite, 95K-5e, 95K-8a', A-12, KZ-7, KZ-10) yielded relatively flat spectra (Fig. 2a) for which we calculated either weighted mean plateau ages or weighted mean ages. All have  $^{40}\text{Ar}/^{36}\text{Ar}$  ratios indistinguishable from or close to atmosphere, indicating that the WMPA is preferable to the isochron age. These samples might be affected by excess Ar, but there is no indication of such from the shapes of the spectra or from the distribution of the measured isotopic ratios.

Another four micas (95K-3 biotite, 95K-5c, 95K-11a, 95K-11c) have more internally discordant spectra (Fig. 2b). In particular, the biotite spectra all have intermediate-temperature steps with anomalously old ages and depressed K/Ca ratios, suggesting that these biotites are chloritized and that these steps are affected by recoil of  $^{39}\text{Ar}$  during irradiation (Lo and Onstott, 1989; Ruffet et al., 1991). It is important to note that biotite and muscovite were both analyzed from sample 95K-3, yet the biotite WMA is older than the muscovite WMA; this hints that the biotite, with a more discordant spectrum, may be affected by excess Ar in addition to recoil.

The two oldest ages ( $529.4 \pm 2.0$  Ma and  $528.3 \pm 1.8$  Ma) of these two groups of samples derive from relatively well-behaved spectra (95K-5e and KZ-10) and are equivalent at the 95% confidence level at  $\sim 529$  Ma. Seven of our eight younger mica ages cluster around  $509.2 \pm 1.7$  Ma (MSWD=4.3), and the subset of four samples with the relatively flat spectra gives a mean of  $507.9 \pm 2.2$  Ma (MSWD=2.4).

Two mica samples from the Kulet area (95K-21f muscovite, KZ-24) have even less well-defined spectra with anomalously low K/Ca ratios for which we provisionally estimate ages of  $495.6 \pm 1.2$  and  $504.7 \pm 1.0$  Ma (Fig. 2c). The isochron for KZ-24 is meaningless, with an  $^{40}\text{Ar}/^{36}\text{Ar}$  ratio of  $239 \pm 21$ . Two other mica samples (95K-2, 95K-21f biotite; not shown) and three hornblendes (Fig. 2d) yielded spectra that have no age significance but indicate the presence of excess  $^{40}\text{Ar}$ .

We also made a concerted effort to obtain an age on a separate of K-bearing diopside (sample 95K-7; Fig. 3). The diopside contains inclusions of K-bearing phases—K-feldspar and probably phengite (Ogasawara et al., 2000)—that are  $< 1\text{-}\mu\text{m}$  thick and 10- to 200- $\mu\text{m}$  long. We infer that the ultrahigh-pressure stage of eclogite recrystallization produced homogeneous K-rich clinopyroxene and that lower P–T annealing resulted in exsolution of the K-feldspar and phengite. As far as we are aware, this is the first report of  $^{40}\text{Ar}/^{39}\text{Ar}$  dating of such a crystal. K-bearing clinopyroxenes hold considerable promise as thermochronometers because they are the only K-bearing phase other than K-feldspar that may not decompose during heating in the resistance furnace until relatively high temperature, conceivably

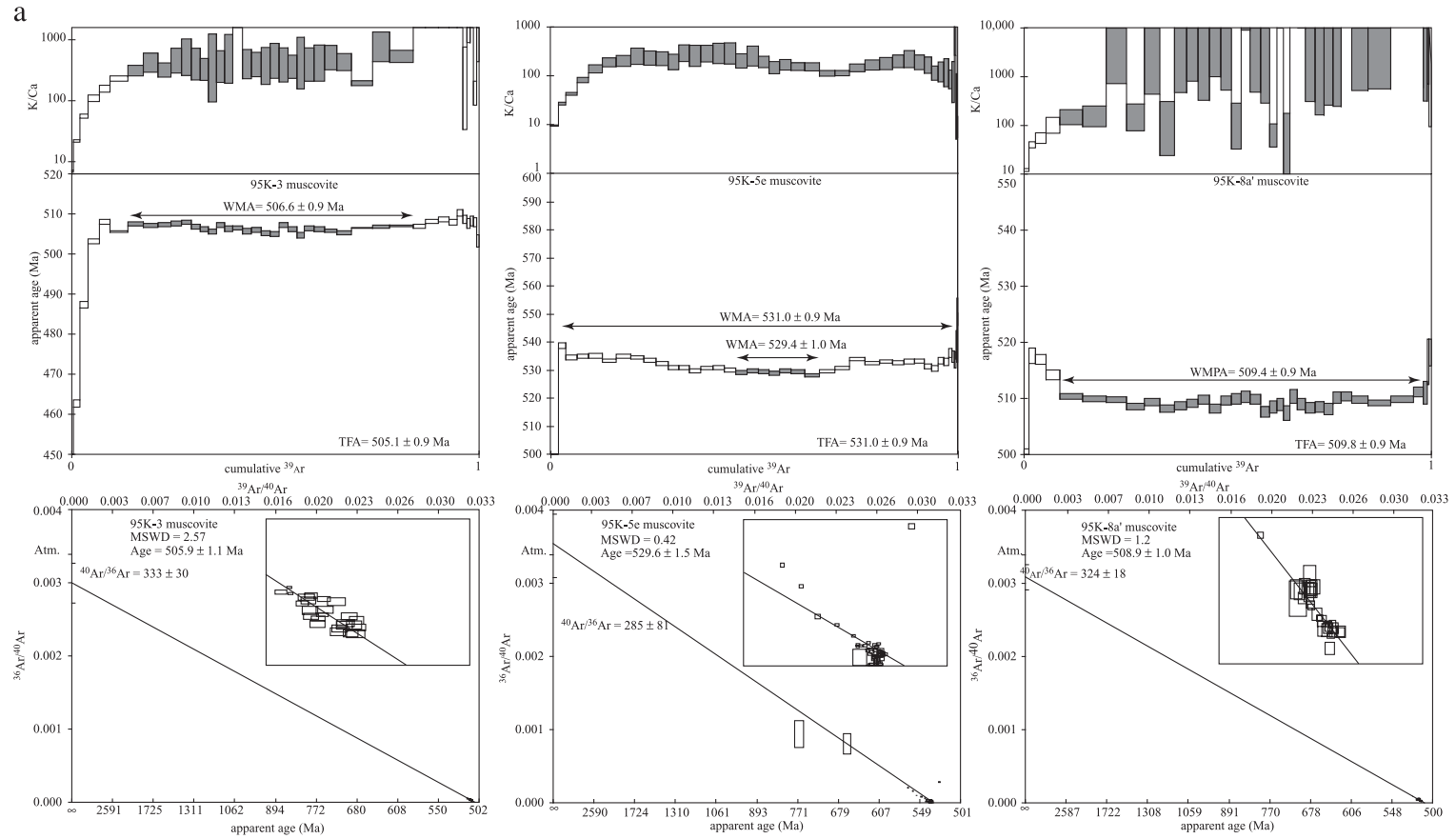


Fig. 2.  $^{40}\text{Ar}/^{39}\text{Ar}$  spectra (step ages do not include error in irradiation parameter, J), K/Ca spectra (maximum value shown is 10,000, beyond which  $^{37}\text{Ar}/^{39}\text{Ar}$  cannot be distinguished from blank), and inverse isochron diagrams for hornblende and mica. Steps used to compute WMPA ages are shown in dark gray. Inset in each isochron diagram shows fit in more detail. (a) Samples with relatively flat spectra. (b) Samples with moderately flat spectra. (c) Samples with least flat spectra. (d) Hornblende separates.

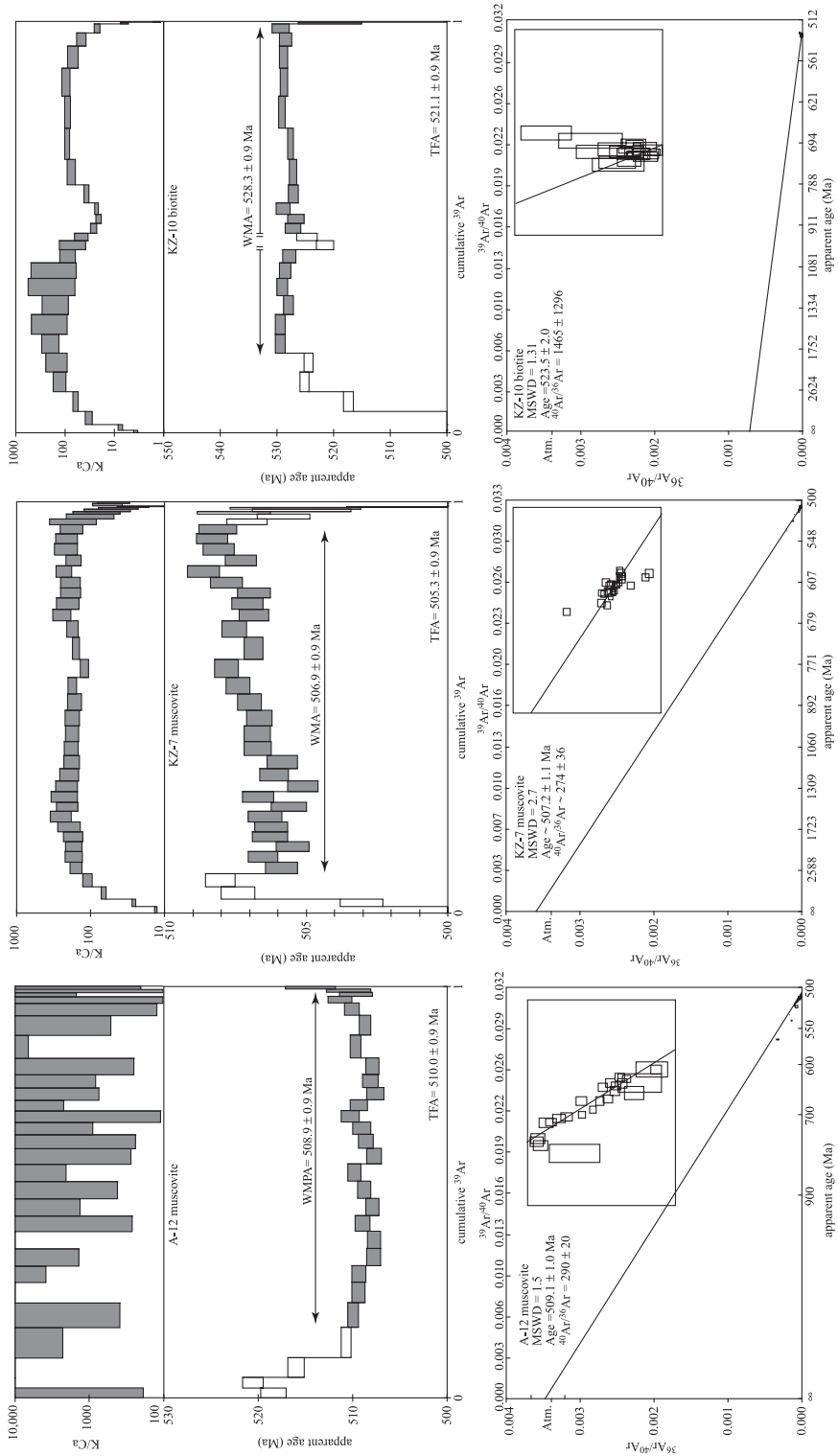


Fig. 2 (continued).

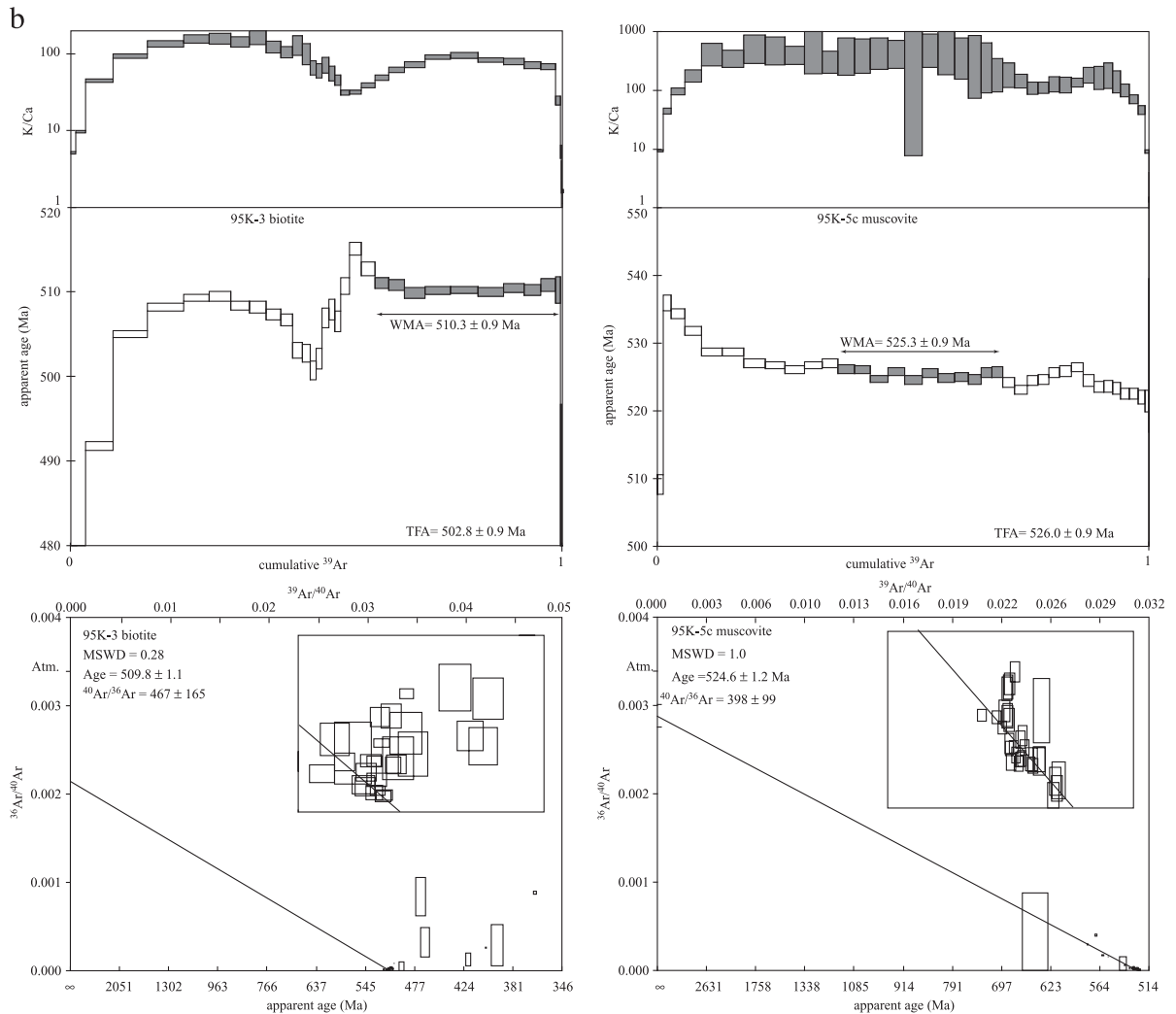


Fig. 2 (continued).

rendering them amenable to multi-domain diffusion analysis (e.g., Lovera et al., 1997). Because we suspected a complex spectrum and hoped to apply multi-domain diffusion analysis, we conducted considerable temperature-cycling steps during the analysis. The K/Ca ratios suggest that the low-temperature steps are derived chiefly from the exsolved phases and that the high-temperature steps comprise gas from dominantly K-bearing pyroxene, respectively (Fig. 3). The spread of isotopic ratios from measurements with relatively low  $^{40}\text{Ar}/^{36}\text{Ar}$  ratios is compatible with an Ar-loss event at  $\sim 450$ – $500$  Ma.

Beyond this, we are unable to interpret the data for the K-bearing diopside.

Shatsky et al. (1999a) reported two  $^{40}\text{Ar}/^{39}\text{Ar}$  spectra from Kumdy–Kol diamond-bearing garnet–biotite gneiss (their sample K83-3); muscovite and biotite gave plateau ages of  $515 \pm 10$  and  $517 \pm 10$  Ma, respectively. Travin (1999) (also reported in Theunissen et al., 2000) conducted a more comprehensive  $^{40}\text{Ar}/^{39}\text{Ar}$  dating program. Four of their samples (17A, 25E, 26C, Ku98-8) from Unit II at Kulet gave ages of 565–635 Ma, prompting Travin to suggest that these samples are affected by excess

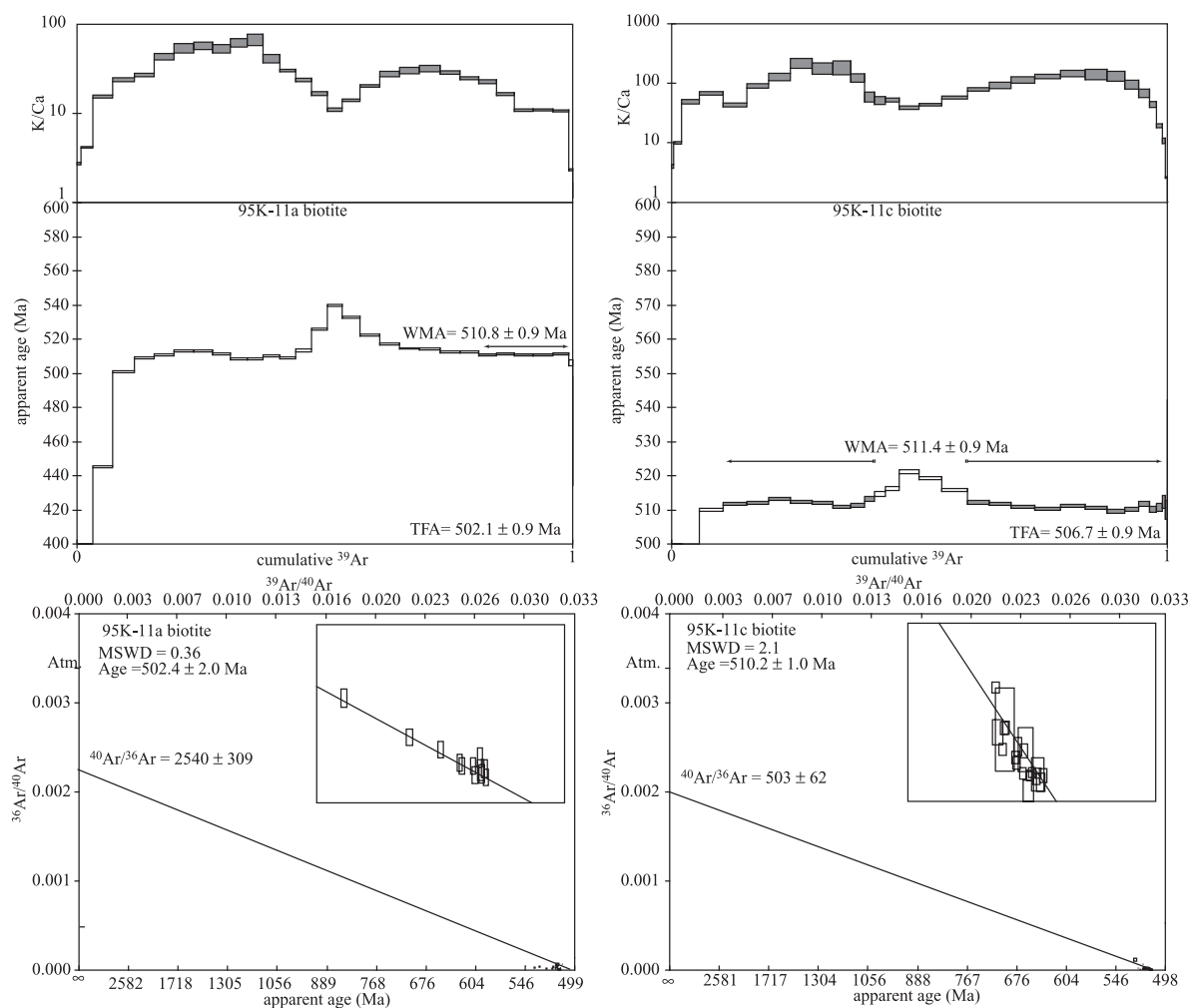


Fig. 2 (continued).

$^{40}\text{Ar}$ . Two other gneiss and schist samples (Ku98-20, Ku98-12) from the same area gave muscovite and biotite plateau ages of  $519.3 \pm 3.6$  and  $521.5 \pm 7.8$  Ma, respectively. Travin also obtained hornblende and muscovite ages from Unit IV (samples 90B and 90D) at Chaglinka of  $516.6 \pm 12.4$  and  $498.1 \pm 4.4$  Ma. The former is equivalent to our  $\sim 508$  Ma samples from Kumdy–Kol and the latter to our  $\sim 500$  Ma samples from the Kulet area. Two cordierite schists (Ku98-2, E-98-8) from the Dault unit gave muscovite and biotite plateau ages of  $396.0 \pm 12.0$  and  $402.0 \pm 10.2$  Ma, respectively (Travin, 1999), indicating cooling  $\sim 100$  Myr later than the bulk of the Kokchetav Massif.

#### 4. Tectonic interpretation

Our new geochronologic data can be integrated with existing geochronology to yield a better constrained exhumation history for the Kokchetav Massif (Fig. 4). First we make the assumption that the Sm/Nd mineral isochron of  $535 \pm 3$  Ma dates the time of eclogite-facies metamorphism in Unit II. While this ingrowth of radiogenic Nd need not have happened at the peak metamorphic conditions of  $780\text{--}1000$  °C,  $100\text{--}180(?)$  km (Okamoto et al., 2000), it nevertheless must have occurred at eclogite-facies pressures. Second, because the amphibolite-facies metamorphism

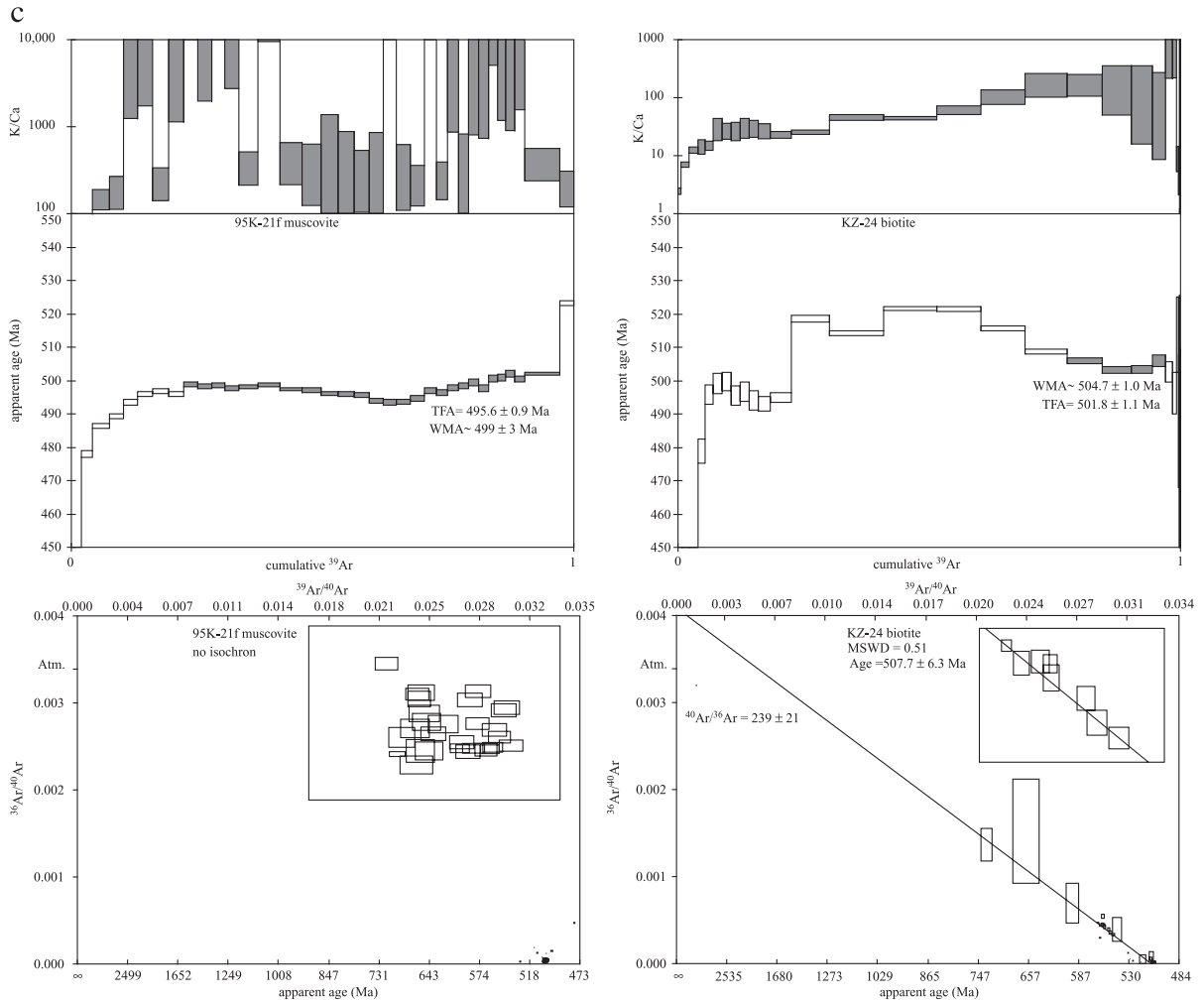


Fig. 2 (continued).

that overprinted the high-pressure minerals at 20- to 40-km depth was likely too hot (570–680 °C) (Masago, 2000; Ota et al., 2000) for Ar retention, the oldest  $^{40}\text{Ar}/^{39}\text{Ar}$  muscovite and biotite ages should indicate when the UHP rocks had been exhumed through the mantle and reached crustal levels. We provisionally interpret the  $\sim 529$  Ma mica ages from samples 95K-5e and KZ-10 as signifying this—in which case the duration of exhumation was  $\sim 6$  Myr. Accordingly, the average vertical rate of exhumation was comparable to plate tectonic rates, at 15–30 km/Myr. The grouping of mica ages around  $\sim 529$

Ma from two different minerals and three different rock types—regardless of whether one chooses WMPA ages or total fusion ages—implies that this conclusion is robust. However, the presence of excess  $^{40}\text{Ar}$  cannot be discounted, and this study should be followed up by additional studies to assess whether these ages are reliable.

The second group of mica ages, at  $\sim 508$  Ma, is a much more clearly defined population composed of a greater number of samples that yield less-disturbed spectra. This group is equivalent in age to the U/Pb SHRIMP determinations of  $507 \pm 8$  Ma that

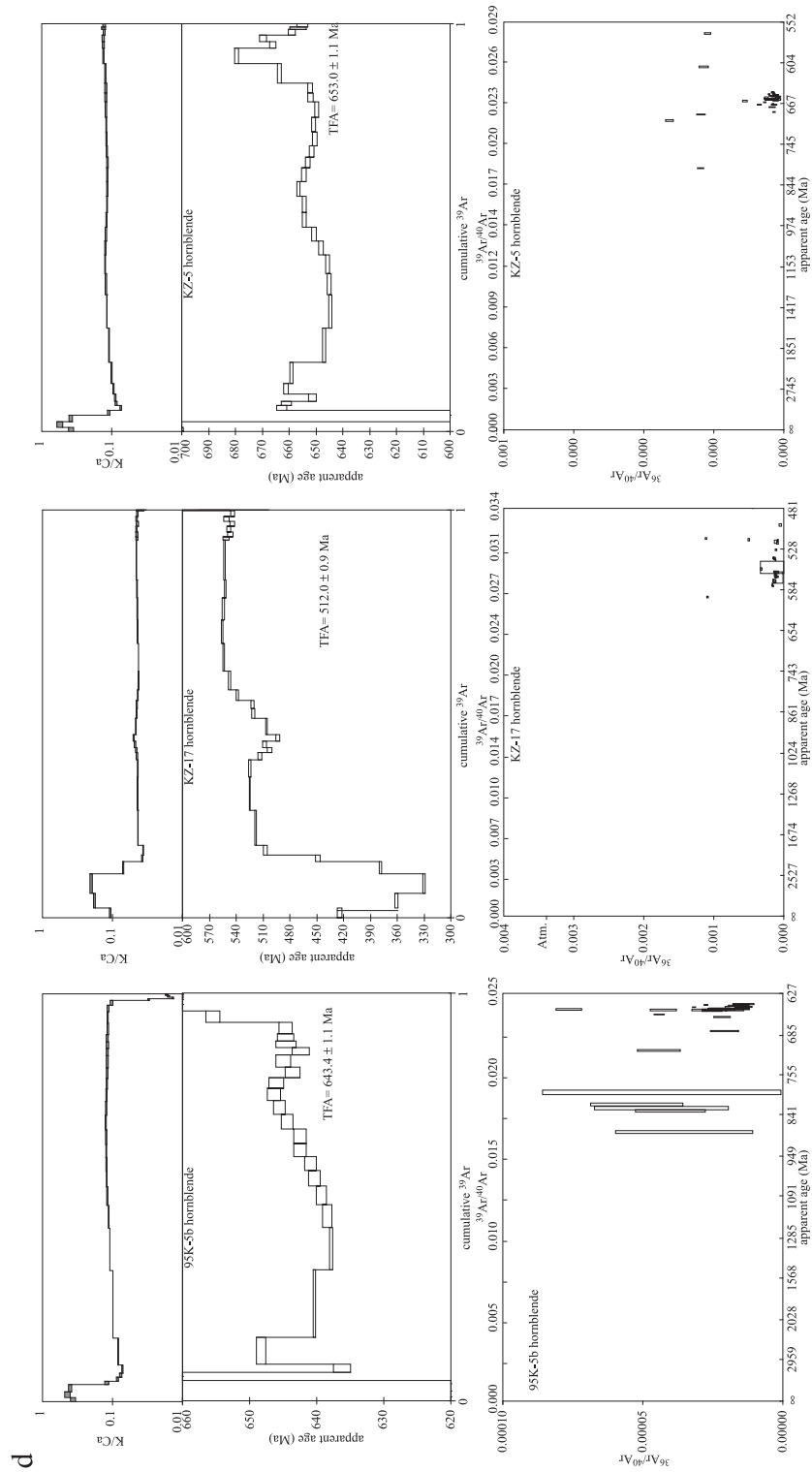


Fig. 2 (continued).

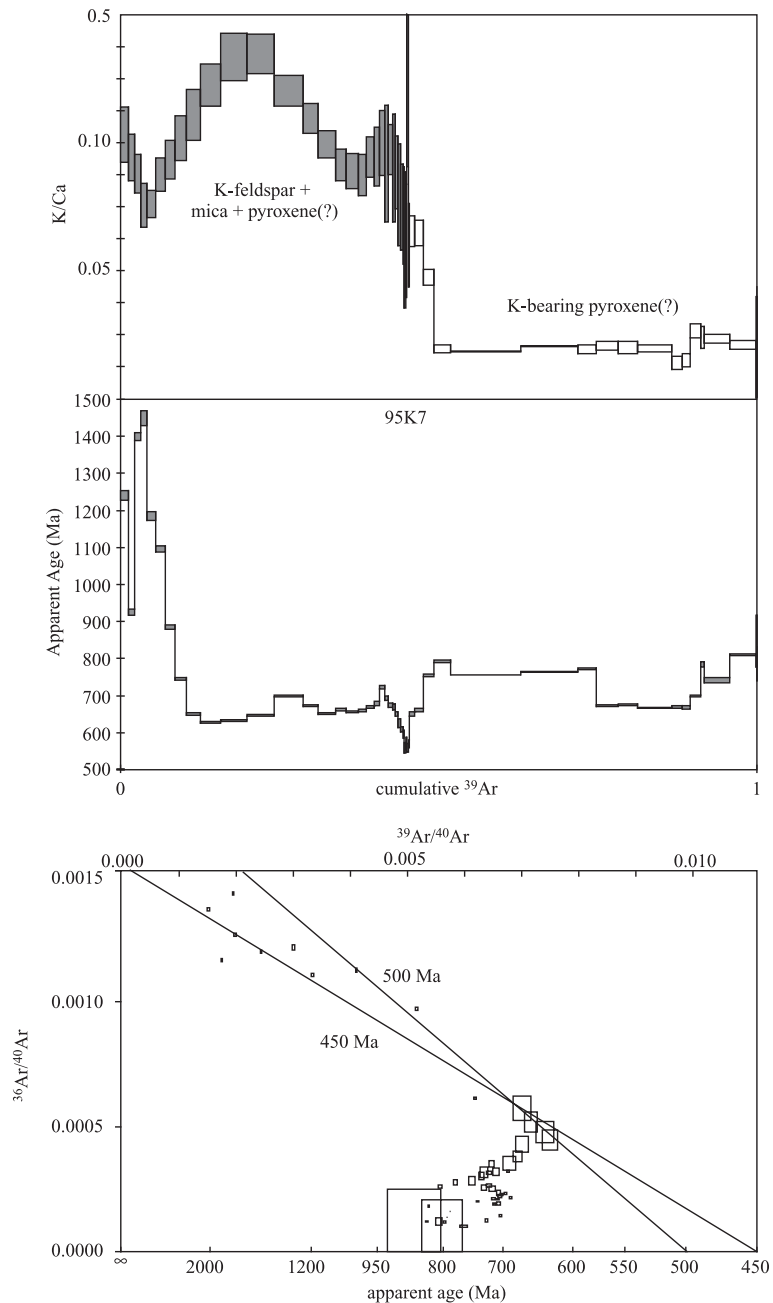


Fig. 3.  $^{40}\text{Ar}/^{39}\text{Ar}$  spectrum, K/Ca spectrum, and inverse isochron for K-bearing diopside separate.

Katayama et al. (2001) obtained from the rims of zircons that contain low-P mineral inclusions such as graphite, quartz, and chlorite. Together, these mica and zircon ages indicate a tectonic event that caused

zircon growth or Pb loss and reset some mica grains to  $\sim 508$  Ma but did not reset other micas in the same area (i.e., the  $\sim 529$  Ma group). The  $\sim 508$  Ma mica samples do not exhibit any systematic difference in

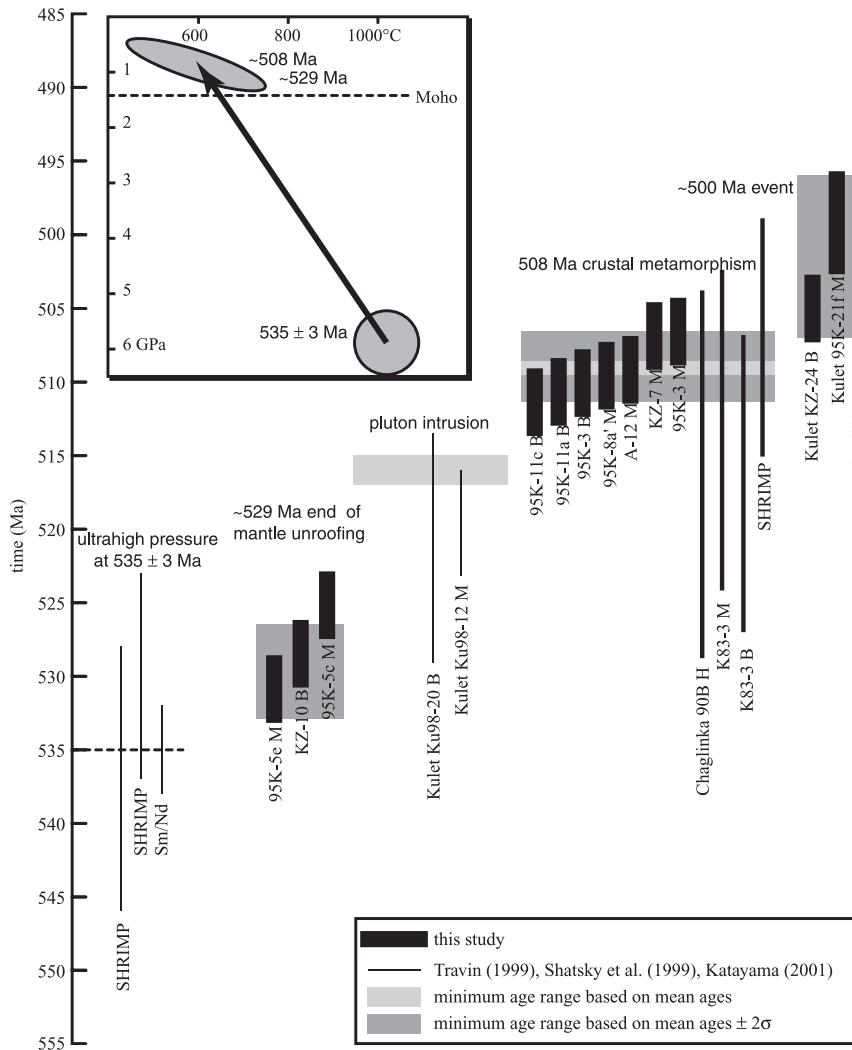


Fig. 4. Summary of extant geochronology for the Kokchetav Massif. Each vertical bar shows the  $2\sigma$  uncertainty of a single age determination. Horizontal gray bars show minimum age ranges of “events”. All samples are from Kumdy–Kol unless otherwise noted as “Sulu–Tjube”, “Chaglinka”, or “Kulet”. “H”, “M”, “B” following sample number indicate hornblende, muscovite, and biotite. Inset P–T diagram after Maruyama and Parkinson (2000).

style or degree of deformation from the ~ 529 Ma mica samples, such that perhaps a brief amphibolite-facies or greenschist-facies event with heterogeneous fluid flow that promoted local reaction is most likely. Other, perhaps, less likely possibilities are that the ~ 508 Ma ages reflect (i) cooling following the regional amphibolite-facies metamorphism mentioned above, (ii) cooling following regional plutonism at 515–517 Ma (Borisova et al., 1995), or (iii) partial Ar loss associated with the intrusion of local 500–505

Ma gabbro–pyroxenite intrusions (Dobretsov et al., 1998).

Katayama et al. (2001) interpreted the same data set, without our  $^{40}\text{Ar}/^{39}\text{Ar}$  ages, as indicating much slower exhumation of the Kokchetav Massif over a 30 Myr timeframe from ~ 537 to ~ 507 Ma. We prefer the interpretation that exhumation of the ultrahigh-pressure rocks through the mantle was finished by 529 Ma, however, because of the mica samples that began to retain radiogenic Ar at that time.

Further measurements of the cooling history and exhumation rate are warranted, however, to see whether this interpretation finds other supporting evidence.

## 5. Conclusions

New  $^{40}\text{Ar}/^{39}\text{Ar}$  data, in conjunction with existing Sm/Nd and U/Pb ages, suggest that the ultrahigh-pressure Kokchetav Massif may have been exhumed from 180-km depth to crustal depths within  $\sim 6$  Myr. The exhumation rate—tens of kilometers per million years—may have been comparable to rates of plate spreading and subduction. The best documentations of similarly fast exhumation rates for other ultrahigh-pressure rocks are the Zermatt–Saas ophiolite (Amato et al., 1999) and the Dora Maira massif (Rubatto and Hermann, 2001).

## Acknowledgements

Thanks to Ikuo Katayama for providing a preprint and to Koen de Jong, Simon Kelley, Gilles Ruffet, and Laura Webb for instructive reviews. Statistical analysis was conducted using ‘Eyesorecon’ by B.R. Hacker and ‘Isoplot’ by K.R. Ludwig. This study was supported by the National Science Foundation.

## References

- Amato, J.M., Johnson, C., Baumgartner, L., Beard, B., 1999. Sm–Nd geochronology indicates rapid exhumation of Alpine eclogites. *Earth Planet. Sci. Lett.* 171, 425–438.
- Arnaud, N.O., Kelley, S., 1995. Evidence for excess Ar during high pressure metamorphism in the Dora-Maira (western Alps, Italy), using a Ultra-Violet Laser Ablation Microprobe  $^{40}\text{Ar}/^{39}\text{Ar}$  technique. *Contrib. Mineral. Petrol.* 121, 1–11.
- Borisova, E., Bibikova, E.V., Dobrzhinetskaya, L.E., Makarov, V.A., 1995. Geochronological study of zircon from Kokchetav diamondiferous area. *Dokl. Akad. Nauk UzSSR* 343, 801–805.
- Brueckner, H.K., Blusztajn, J., Bakun-Czubarow, N., 1996. Trace element and Sm–Nd ‘age’ zoning in garnets from peridotites of the Caledonian and Variscan Mountains and tectonic implications. *J. Metamorph. Geol.* 14, 61–73.
- Calvert, A.T., Gans, P.B., Amato, J.M., 1999. Diapiric ascent and cooling of a sillimanite gneiss dome revealed by  $^{40}\text{Ar}/^{39}\text{Ar}$  thermochronology: the Kigluaik Mountains, Seward Peninsula, Alaska. In: Ring, U., Brandon, M.T., Lister, G., Willett, S. (Eds.), *Exhumation Processes: Normal Faulting, Ductile Flow, and Erosion*. Geological Society of London, London, pp. 205–232.
- Claoue-Long, J.C., Sobolev, N.V., Shatsky, V.S., Sobolev, A.V., 1991. Zircon response to diamond-pressure metamorphism in the Kokchetav Massif, USSR. *Geology* 19, 710–713.
- Dobretsov, N.L., Theunissen, K., Smimova, L.V., 1998. Structural and geodynamic evolution of the diamondiferous metamorphic rocks of the Kokchetav Massif. *Russ. Geol. Geophys.* 39, 1631–1652.
- El-Shazly, A.E., Broecker, M.S., Hacker, B.R., Calvert, A.T., 2001. Formation and exhumation of blueschists and eclogites from NE Oman: new constraints from Rb–Sr and  $^{40}\text{Ar}/^{39}\text{Ar}$  dating. *J. Metamorph. Geol.* 19, 233–248.
- Foland, K.A., 1983.  $^{40}\text{Ar}/^{39}\text{Ar}$  incremental heating plateaus for biotites with excess argon. *Chem. Geol.* 1, 3–21.
- Georgis, D., Cosca, M., Li, S., 2000. Distribution and significance of extraneous argon in UHP eclogite (Sulu terrain, China): insight from in situ  $^{40}\text{Ar}/^{39}\text{Ar}$  UV-laser ablation analysis. *Earth Planet. Sci. Lett.* 181, 605–615.
- Hacker, B.R., Wang, Q.C., 1995. Ar/Ar geochronology of ultrahigh-pressure metamorphism in central China. *Tectonics* 14, 994–1006.
- Hacker, B.R., Ratschbacher, L., Webb, L., Ireland, T., Walker, D., Dong, S., 1998. U/Pb zircon ages constrain the architecture of the ultrahigh-pressure Qinling–Dabie Orogen, China. *Earth Planet. Sci. Lett.* 161, 215–230.
- Harrison, T.M., McDougall, I., 1981. Excess  $^{40}\text{Ar}$  in metamorphic rocks from Broken Hill, New South Wales: implications for  $^{40}\text{Ar}/^{39}\text{Ar}$  age spectra and the thermal history of the region. *Earth Planet. Sci. Lett.* 55, 123–149.
- Ishikawa, M., Kaneko, Y., Anma, R., Yamamoto, H., 2000. Sub-horizontal boundary between ultrahigh-pressure and low-pressure metamorphic units of the Sulu–Tjube area of the Kokchetav Massif, Kazakhstan. *Isl. Arc* 9, 317–327.
- Kaneko, Y., Maruyama, S., Terabayashi, M., Yamamoto, H., Ishikawa, M., Anma, R., Parkinson, C.D., Ota, T., Nakajima, Y., Katayama, I., Yamamoto, J., Yamauchi, K., 2000. Geology of the Kokchetav UHP-HP metamorphic belt, northern Kazakhstan. *Isl. Arc* 9, 264–283.
- Katayama, I., Zayachkovsky, A.A., Maruyama, S., 2000. Prograde pressure-temperature records from inclusions in zircons from ultrahigh-pressure–high-pressure rocks of the Kokchetav Massif, northern Kazakhstan. *Isl. Arc* 9, 417–427.
- Katayama, I., Maruyama, S., Parkinson, C.D., Terada, K., Sano, Y., 2001. Ion microprobe U–Pb zircon geochronology of peak and retrograde stages of ultrahigh-pressure metamorphic rocks from the Kokchetav Massif, northern Kazakhstan. *Earth Planet. Sci. Lett.* 188, 185–198.
- Li, S., Wang, S., Chen, Y., Liu, D., Qiu, J., Zhou, H., Zhang, Z., 1994. Excess argon in phengite from eclogite: Evidence from the dating of eclogite minerals by the Sm–Nd, Rb–Sr and  $^{40}\text{Ar}/^{39}\text{Ar}$  methods. *Chem. Geol.* 112, 343.
- Lo, C.H., Onstott, T.C., 1989.  $^{39}\text{Ar}$  recoil artifacts in chloritized biotite. *Geochim. Cosmochim. Acta* 53, 2697–2711.
- Lovera, O.M., Grove, M., Harrison, T.M., Mahon, K.I., 1997. Systematic analysis of K-feldspar  $^{40}\text{Ar}/^{39}\text{Ar}$  step heating results: I.

- Significance of activation energy determinations. *Geochim. Cosmochim. Acta* 61, 3171–3192.
- Maruyama, S., Parkinson, C.D., 2000. Overview of the geology, petrology and tectonic framework of the high-pressure–ultra-high-pressure metamorphic belt of the Kokchetav Massif, Kazakhstan. *Isl. Arc* 9, 439–455.
- Masago, H., 2000. Metamorphic petrology of the Barchi–Kol metabasites, western Kokchetav ultrahigh-pressure–high-pressure massif, northern Kazakhstan. *Isl. Arc* 9, 358–378.
- Ogasawara, Y., Ohta, M., Fukasawa, K., Katayama, I., Maruyama, S., 2000. Diamond-bearing and diamond-free metacarbonate rocks from Kumdy–Kol in the Kokchetav Massif, northern Kazakhstan. *Isl. Arc* 9, 400–416.
- Okamoto, K., Liou, J.G., Ogasawara, Y., 2000. Petrology of the diamond-grade eclogite in the Kokchetav Massif, northern Kazakhstan. *Isl. Arc* 9, 379–399.
- Ota, T., Terabayashi, M., Parkinson, C.D., Masago, H., 2000. Thermobaric structure of the Kokchetav ultrahigh-pressure–high-pressure massif deduced from a north–south transect in the Kulet and Saldat–Kol regions, northern Kazakhstan. *Isl. Arc* 9, 328–357.
- Parkinson, C.D., 2000. Coesite inclusions and prograde compositional zonation of garnet in whiteschist of the HP-UHPM Kokchetav Massif, Kazakhstan: a record of progressive UHP metamorphism. *Lithos* 52, 215–233.
- Rex, D.C., Guise, P.G., Wartho, J.A., 1993. Disturbed  $^{40}\text{Ar}/^{39}\text{Ar}$  spectra from hornblendes: thermal loss or contaminations? *Chem. Geol.* 103, 271–281.
- Rubatto, D., Hermann, J., 2001. Exhumation as fast as subduction? *Geology* 29, 3–6.
- Ruffet, G., Féraud, G., Amouric, M., 1991. Comparison of  $^{40}\text{Ar}/^{39}\text{Ar}$  conventional and laser dating of biotites from the North Trégor Batholith. *Geochim. Cosmochim. Acta* 55, 1675–1688.
- Scailliet, S., 1998. K–Ar ( $^{40}\text{Ar}/^{39}\text{Ar}$ ) geochronology of ultrahigh pressure rocks. In: Hacker, B.R., Liou, J.G. (Eds.), *When Continents Collide: Geodynamics and Geochemistry of Ultrahigh-Pressure Rocks*. Kluwer Academic Publishers, Dordrecht, pp. 161–201.
- Shatsky, V.S., Jagoutz, E., Kozmenko, O.A., Blinichik, T.M., Sobolev, N., 1993. Age and genesis of eclogites from the Kokchetav Massif. *Russ. Geol. Geophys.* 34, 40–50.
- Shatsky, V.S., Jagoutz, E., Kozmenko, O.A., Parkhomenko, V.S., Troesch, M., Sobolev, N., 1999a. Geochemistry and age of ultrahigh-pressure rocks from the Kokchetav Massif (northern Kazakhstan). *Contrib. Mineral. Petrol.* 137, 185–205.
- Shatsky, V.S., Jagoutz, E., Kozmenko, O.A., Sobolev, N., 1999b. The age of the UHP metamorphism and protoliths. In: Dobretsov, N.L., Sobolev, N.V., Shatsky, V.S. (Eds.), *Fourth International Eclogite Symposium Field Guide Book*. United Institute of Geology, Geophysics and Mineralogy, Siberian Branch of Russian Academy of Sciences, Novosibirsk, pp. 50–52.
- Sobolev, N.V., Shatsky, V.S., Shatskiy, V.S., 1990. Diamond inclusions in garnets from metamorphic rocks; a new environment for diamond formation. *Nature* 343, 742–746.
- Terabayashi, M., 1999. The Daultet metamorphism: a contact metamorphism by solid intrusion of UHP-HP metamorphic slab. *Superplume International Workshop Abstracts*, 261–273.
- Theunissen, K., Dobretsov, N.L., Korsakov, A., Travin, A., Shatsky, V.S., Smirnova, L., Boven, A., 2000. Two contrasting petrotectonic domains in the Kokchetav megamélange (north Kazakhstan): difference in exhumation mechanisms of ultrahigh-pressure crustal rocks, or a result of subsequent deformation? *Isl. Arc* 9, 284–303.
- Tonarini, S., Villa, I.M., Oberli, F., Meier, M., Spencer, D.A., Pogonante, U., Ramsay, J.G., 1993. Eocene age of eclogite metamorphism in Pakistan Himalaya: implications for India–Eurasia collision. *Terra Nova* 5, 13–20.
- Travin, A., 1999. Ar/Ar geochronology of the Kokchetav megamélange. In: Dobretsov, N.L., Sobolev, N.V., Shatsky, V.S. (Eds.), *Fourth International Eclogite Field Symposium Guide to the Diamondiferous and High Pressure Metamorphic Rocks of Kokchetav Massif (Northern Kazakhstan)*. United Institute of Geology, Geophysics and Mineralogy, Siberian Branch of Russian Academy of Sciences, Novosibirsk, pp. 52–56.
- Wijbrans, J.R., McDougall, I., 1986.  $^{40}\text{Ar}/^{39}\text{Ar}$  dating of white micas from an Alpine high-pressure metamorphic belt on Naxos (Greece): the resetting of the argon isotopic system. *Contrib. Mineral. Petrol.* 93, 187–194.
- Yamamoto, H., Ishikawa, M., Anma, R., Kaneko, Y., 2000. Kinematic analysis of ultrahigh-pressure–ultrahigh-pressure metamorphic rocks in the Chaglinka–Kulet area of the Kokchetav Massif, Kazakhstan. *Isl. Arc* 9, 304–316.